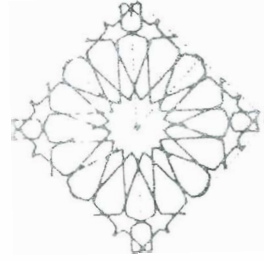




المؤتمر العلمي الدولي الثاني  
لكلية الهندسة - جامعة الأزهر

٩١ - ٩٤ ديسمبر ١٩٩١

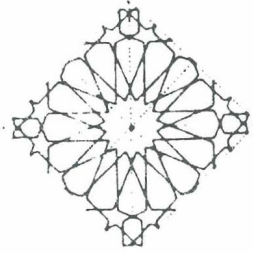


كلية الهندسة  
جامعة الأزهر

المجلد الخامس  
هندسة كهربية  
جزء أول



AL-AZHAR ENGINEERING SECOND  
INTERNATIONAL CONFERENCE  
December 21-24, 1991



**AEC '91**  
Faculty of Engineering  
Al-Azhar University

VOLUME V

ELECTRICAL ENGINEERING

ELECTRICAL POWER AND MACHINES

Switching Problems of Accelerating Asynchronous Generator Using Magnetic Switch and Extra Stator Resistances. W. Deleroi and J.B. Woudstra .....	265
A Solid State Dynamic Braking - DC Injection Scheme for Isolated Induction Generators in Stand Alone Wind Energy Systems. R.M. Hilloowala and A.M. Sharaf .....	277
Dynamic Stability of a Wind-Driven Induction Generator Under Varying Loading Conditions. E.S. Abdin .....	289
Synchronous Machine Control Using a Two Level Algorithm with Partial Feedbacks. F. Bendary and F.A. Khalifa .....	300
Optimal Speed Control of DC Series Motor Controlled by Chopper Circuit. Mohamed M.M. Negm .....	310
Unified Model of Speed and Current Controlled D.C. Motor Fed by Thyristor Chopper. F. Gibril and A.S. Abdel-Ghaffar .....	321
Dynamic Responses of D.C. Chopper-Controlled Series Motor. F.M. EL-Khouly, F. Gibril, A.S. Abdel-Ghaffar and A.A. Mohamed .....	340
A Two-Levels Weighted Least Squares Estimation. Mosa s. Deyab .....	353
Identification and Network Reduction Algorithm for Dynamic Equivalent of Power Systems. Mahdi M.M. El-Arini .....	373
Microprocessor-Controlled Separately-Excited DC Motor Drive. S. Amer, A.M. Zaki, S.Wahsh and A.A. El-Sattar ....	383
The Acceleration Characteristics of the Trapezoidally Railed Linear Homopolar Synchronous Motor as Compared to the Zig-Zag Version for Maglev Applications. S.M. Al-Kasimi and A.O. BaQubas .....	392
Force Computation on Windings of Transformers Using a Nonlinear Two Dimension Finite Element Method. A.M. El-Khatib .....	410



THE ACCELERATION CHARACTERISTICS OF THE TRAPIZOIDALLY RAILED  
LINEAR HOMOPOLAR SYNCHRONOUS MOTOR AS COMPARED TO  
THE ZIG-ZAG VERSION FOR MAGLEV APPLICATIONS

S.M.Al-Kasim\* and A.O.BaQubas\*\*

\* Assistant Prof., Elec. Eng. Dept., Umm-El-Qura Univ., Makkah, Saudi Arabia.

\*\* BSc Student, Elec. Eng. Dept., Umm-El-Qura Univ., Makkah, Saudi Arabia.

ABSTRACT

The Zig-Zag Linear Homopolar Synchronous Motor, ZZLHSM, is a machine that provides a combined lift and thrust for maglev vehicles. A maglev vehicle is a vehicle that is supported by magnetic attraction between controlled electromagnets fixed to its chassis and a pair of iron tracks. The magnet of ZZLHSM is U-shaped and acts as a two-pole machine in which each pole is split into two sub-poles. Each sub-pole is surrounded by a coil fed by an inverter such that the field could be distorted among the four sub-poles. The rail of the ZZLHSM is zig-zag shaped and will move relative to the sub-poles to minimise reluctance, hence propulsion is obtained. The ZZLHSM machine version was modified by changing the shape of the rail to a trapezoidal one, and hence obtaining a Trapezoidally Railed Linear Homopolar Synchronous Motor, TRLHSM.

This paper describes in theory the acceleration characteristics of the TRLHSM machine version that could be used for maglev transport utilizing integrated lift & thrust. It first establishes the basic principle of operation whereby the various machine relationships are derived for TRLHSM. Few assumptions are made before finding out these relationships which include: the relationships of fluxes, flux densities, vertical force, horizontal force, open circuit voltages, vertical & horizontal accelerations. Maximum thrusting conditions are then found.

A review is then made for the ZZLHSM version with same winding and excitation conditions, whereby the corresponding relationships are briefed.

The paper concludes with a comparison between the characteristics of TRLHSM and ZZLHSM.

December 21-24, 1991

THE TRAPIZOIDALLY RAILED  
MOTOR AS COMPARED TO  
MAGLEV APPLICATIONS

Abbas\*\*

Umm Al-Qura Univ., Makkah, Saudi Arabia.

King Fahd Univ., Makkah, Saudi Arabia.

ZZLHSM, is a machine that provides a maglev vehicle is a vehicle that is supported by two sets of electromagnets fixed to its chassis. The rail is U-shaped and acts as a two-pole machine. Each sub-pole is surrounded by a coil. The field is forced through the sub-poles. The ZZLHSM machine version was modified by adding a trapezoidal rail and hence obtaining a Trapezoidally Railed Linear Homopolar Synchronous Motor (TRLHSM).

Characteristics of the TRLHSM machine including integrated lift & thrust. It first the various machine relationships are studied before finding out these relationships. The relationships studied are vertical force, horizontal force, and thrusting conditions. Maximum thrusting conditions are studied.

With the same winding and excitation conditions, the characteristics of TRLHSM and ZZLHSM are compared.

Keywords: Trapezoidal, Linear, Homopolar, Synchronous, Machine, Maglev, Suspension, Propulsion & Transportation.

KEYWORDS

Fig-Zag, Trapezoidal, Linear, Homopolar, Synchronous, Machine, Maglev, Suspension, Propulsion & Transportation.

INTRODUCTION

Fig. 1 shows the ZZLHSM magnet within a maglev vehicle boggie. The main poles of ZZLHSM are excited by field current through dc coils. Each of the main poles is split into two sub-poles that are surrounded by ac coils. McLean[1,2] and West[1] have chosen a rail shape shown in Fig. 2a. Hence, with the ac coils around sub-poles excited such that the field is forced through sub-poles 1&3, the rail will move assuming constant air gap,  $z$ , to link sub-poles 1&3. When field is forced through sub-poles 2&4, the rail will move again to link sub-poles 2&4. As the switching of sub-pole coil-excitations synchronizes to rail position, a continuous motion is obtained. The ZZLHSM is unable, due to symmetry, to start motion when the rail completely links sub-poles 1&3 or sub-poles 2&4 at a stop. This may be avoidable by another ZZLHSM pair placed half pole-pitch away.

Now for the same magnet, if a trapezoidally shaped rail like the one shown in Fig. 2b is used, the ac coils around sub-poles can be excited to force field through sub-poles 1&3. Hence, the rail will move assuming constant air gap,  $z$ , to link sub-poles 1&3. The field is then forced through sub-poles 2&3. Hence, pulling the rail to link sub-poles 2&3. Forced through sub-poles 2&4, the field then pulls the rail to link sub-poles 2&4. Finally, when field is forced into sub-poles 1&4, the rail will move to link them both. This completes one cycle and as excitations of sub-pole ac coils are synchronized to rail position, a continuous motion is obtained.

This Trapezoidally Railed Linear Homopolar Synchronous Motor, TRLHSM, is noted to have no symmetry position throughout its cycle. Hence, no need for a starter exists. Another feature is that the switching frequency is half that of the ZZLHSM for same speed, since the rail cycle length of the TRLHSM is twice that of the ZZLHSM.

NOTATIONS

The symbols used in this paper are listed below:

- $A$  sub-pole surface area
- $A_i, A'_i$  overlap area of sub-pole  $i$  in TRLHSM, ZZLHSM respectively
- $a_{hp}, a'_{hp}$  horizontal pulsating acceleration relative to gravity in TRLHSM, ZZLHSM
- $a'_{hpz}$  maximum horizontal pulsating acceleration relative to gravity
- $a_{hs}, a'_{hs}$  horizontal steady acceleration relative to gravity in TRLHSM, ZZLHSM

$a_{hss}, a'_{hss}$  maximum horizontal steady acceleration relative to gravity in TRLHSM, ZZLHSM  
 $a_{vs}, a'_{vs}$  vertical pulsating acceleration relative to gravity in TRLHSM, ZZLHSM  
 $a_{vps}, a'_{vps}$  maximum vertical pulsating acceleration relative to gravity in TRLHSM, ZZLHSM  
 $B_i, B'_i$  flux density over sub-pole  $i$  in TRLHSM, ZZLHSM  
 $E_X, E'_X$  open circuit induced voltage at phase X coil terminals in TRLHSM, ZZLHSM  
 $F_h, F'_h$  horizontal thrust force in TRLHSM, ZZLHSM  
 $F_v, F'_v$  vertical lift force in TRLHSM, ZZLHSM  
 $\phi_{si}$  TRLHSM flux due to  $m_i$  which leaves sub-pole  
 $\phi_{ij}$  TRLHSM flux due to  $m_i$  which leaves sub-pole  $i$  to sub-pole  $j$   
 $\phi_k, \phi'_k$  flux due to all sub-polar mmfs that leaves sub-pole  $k$  in TRLHSM, ZZLHSM  
 $i'_X$  current flowing in phase X ac coils of TRLHSM, ZZLHSM  
 $I_D$  current flowing in the field of TRLHSM dc coils  
 $\lambda_p, \lambda'_p$  peak flux linkage per ac coil in TRLHSM, ZZLHSM  
 $\lambda_n, \lambda'_n$  flux linkage of ac coil around sub-pole  $n$  in TRLHSM, ZZLHSM  
 $M_D, M'_D$  net dc mmf excitation of field winding per pole in TRLHSM, ZZLHSM  
 $\bar{M}_D, \bar{M}'_D$  optimum  $M_D, M'_D$  values for maximum thrust  
 $m_X, m'_X$  ac mmf of phase X armature winding per sub-pole in TRLHSM, ZZLHSM  
 $m, m'$  peak values of ac mmf excitation of any phase per sub-pole in TRLHSM,  
 $\bar{m}, \bar{m}'$  optimum  $m, m'$  values for maximum thrust  
 $m_j, m'_j$  resultant mmf excitations around sub-pole  $j$  in TRLHSM, ZZLHSM  
 $\mu_0$  permeability of air  
 $N$  number of turns of ac coil around any sub-pole  
 $N_D$  number of turns of dc coil around any pole  
 $\rho$  pole pitch  
 $T, T'$  time period to complete one cycle in TRLHSM, ZZLHSM  
 $t$  time starting zero when rail completely links sub-poles 1&3

$\theta, \theta'$  phase angles of ac excitations in  $\zeta\zeta$   
 $\bar{\theta}$  optimum phase angles at maximum  
 $\bar{\theta}_+, \bar{\theta}'_+$  optimum phase angles at maximum  
 $\bar{\theta}_-, \bar{\theta}'_-$  optimum phase angles at maximum  
 $u$  speed of rail relative to magnet  
 $W$  weight of supported boggie  
 $\omega, \omega'$  angular frequency of ac supply in T.  
 $z$  energized air gap

#### ASSUMPTIONS

For simplicity, the following assumptions were

1. All sub-poles have the same surface area.
2. AC coils around sub-poles are identical.
3. Width of slot in the main poles is negligible.
4. Fringing and leakage are negligible.
5. Steel and copper losses are negligible.
6. Air gap,  $z$ , is homogeneous over the sub-pole surface.
7. The energized air-gap faces equal area of net pole surface below it throughout the motion 3 above. The rail of TRLHSM, for example in Fig.3. Here, the total area above or below the rail is the sum of the rectangle area and the triangle area, which is constant and equals the sub-pole area.
8. The energized area per pole is composed of one of the two adjacent sub-poles with the flux density varying sinusoidally between zero and  $A$ .
9. Speed of motor relative to track,  $u$ , is constant.
10. Track structure is rigid.
11. The motor does no rotation.

relative to gravity in TRLHSM, ZZLHSM  
 o gravity in TRLHSM, ZZLHSM  
 relative to gravity in TRLHSM, ZZLHSM  
 L, ZZLHSM  
 . coil terminals in TRLHSM, ZZLHSM  
 LHSM  
 b-pole i  
 b-pole i to sub-pole j  
 es sub-pole 6 in TRLHSM, ZZLHSM  
 RLHSM, ZZLHSM  
 dc coils  
 A, ZZLHSM  
 in TRLHSM, ZZLHSM  
 per pole in TRLHSM, ZZLHSM  
 thrust  
 er sub-pole in TRLHSM, ZZLHSM  
 hase per sub-pole in TRLHSM, ZZLHSM  
 ast  
 ole j in TRLHSM, ZZLHSM  
 b-pole  
 ole  
 LHSM, ZZLHSM  
 links sub-poles 1&3

$\theta, \theta'$  phase angles of ac excitations in TRLHSM, ZZLHSM  
 $\bar{\theta}, \bar{\theta}'$  optimum phase angles at maximum thrust conditions in TRLHSM, ZZLHSM  
 $\bar{\theta}_+, \bar{\theta}'_+$  optimum phase angles at maximum accelerations in TRLHSM, ZZLHSM  
 $\bar{\theta}_-, \bar{\theta}'_-$  optimum phase angles at maximum deceleration in TRLHSM, ZZLHSM  
 $u$  speed of rail relative to magnet  
 $W$  weight of supported boggie  
 $\omega, \omega'$  angular frequency of ac supply in TRLHSM, ZZLHSM  
 $z$  energized air gap

ASSUMPTIONS

For simplicity, the following assumptions were made in the analysis to come.

1. All sub-poles have the same surface area,  $A$ .
2. AC coils around sub-poles are identical.
3. Width of slot in the main poles is negligible.
4. Fringing and leakage are negligible.
5. Steel and copper losses are negligible.
6. Air gap,  $z$ , is homogeneous over the sub-poles.
7. The energized air-gap faces equal areas both at rail surface above it and at magnet pole surface below it throughout motion. This is justified in view of assumption 3 above. The rail of TRLHSM, for instance, overlaps with its poles as shown in Fig. 3. Here, the total area above or below energization throughout motion is the sum of the rectangle area and the parallelogram area. This sum is seen to be constant and equals the sub-polar area,  $A$ .
8. The energized area per pole is composed of two portions. Each portion belongs to one of the two adjacent sub-poles within the main pole and is assumed to vary sinusoidally between zero and  $A$ .
9. Speed of motor relative to track,  $u$ , is constant.
10. Track structure is rigid.
11. The motor does no rotation.

12. The motor force is composed of **two** components only, namely, along gravity line and along direction of motion. Although some force component in the third direction is exerted, it will be ignored.
13. Field mmf excitations are constants.
14. Flux linkage for any ac coil varies sinusoidally between a minimum of zero when its sub-pole is fully uncoupled to rail and a maximum when its sub-pole is fully coupled to rail.
15. AC coils are fed with sinusoidal ac current phase-locked to rail.
16. Windage, friction and other drag forces are ignored.

### THEORETICAL ANALYSIS OF TRLHSM PERFORMANCE

#### Coil Connections for TRLHSM

When the rail of TRLHSM moves in the direction indicated in Fig. 2b, flux linkages of ac coils will assume linear segments and can be approximated to sinusoidal variation as shown in Fig. 4a. Note that  $\lambda_1$  &  $\lambda_2$  vary in-phase with each other and that  $\lambda_3$  &  $\lambda_4$  also vary in-phase with each other but in quadrature lag with  $\lambda_1$  &  $\lambda_2$  variations. The period of these variations is given by:

$$T = \frac{4p}{u} \quad (1)$$

with angular frequency,  $\omega$ , given by:

$$\omega = \frac{\pi u}{2p} \quad (2)$$

Hence, to obtain maximum variation in flux linkage per phase, the ac coils are connected as shown in Fig. 5a. Note that phase A leads B by a quarter of a cycle and that the dc coils are connected so as to build **constructive flux** components.

#### Magnetic Sub - polar Excitations for TRLHSM

Each of the sub-poles in Fig. 5a could be considered excited with two components dc of:

$$M_D = N_D I_D \quad (3)$$

and ac of:

$$m_A(t) = N i_A(t) = m \cos(\omega t + \theta) \quad (4)$$

or :

$$m_B(t) = N i_B(t) = m \sin(\omega t + \theta)$$

Using Fig. 5a and denoting  $m_1, m_2, m_3$  and  $m_4$  to sub-poles 1, 2, 3 and 4 respectively, with positive pole, then:

$$m_1(t) = -M_D - m_A(t)$$

$$m_2(t) = -M_D + m_A(t)$$

$$m_3(t) = M_D + m_B(t)$$

$$m_4(t) = M_D - m_B(t)$$

#### Energized Sub - polar Areas for TRLHSM

With  $A_1, A_2, A_3$  and  $A_4$  defined as above, then the area of sub-pole 1 during the rail motion indicated in Fig. 2 is constant and equals  $A$ .

For simplicity, these trapezoidal variations are approximated to a minimum of zero as shown by the dotted lines. These approximations are:

$$A_1(t) = (A/2)[1 + \cos(\omega t - \theta)]$$

$$A_2(t) = (A/2)[1 - \cos(\omega t - \theta)]$$

$$A_3(t) = (A/2)[1 + \cos(\omega t - \theta)]$$

$$A_4(t) = (A/2)[1 - \cos(\omega t - \theta)]$$

This approximation will give a maximum deviation of 15%. However, the sum of areas constituting portion of the rail is constant and equals  $A$ .

#### Magnetic Sub - polar Fluxes for TRLHSM

Let  $\phi_{11}, \phi_{12}, \phi_{13}, \phi_{14}, \phi_{21}, \phi_{22}, \phi_{23}, \phi_{24}, \phi_{31}, \phi_{32}, \phi_{33}, \phi_{34}, \phi_{41}, \phi_{42}, \phi_{43}, \phi_{44}$  be the flux linkages of the sub-poles as shown above. Hence, each of  $m_1, m_2, m_3$  and  $m_4$  mmfs is similar to that shown in Fig. 6. Hence:

$$\phi_{11}(t) = \frac{\mu_0 A_1 m_1 (\bar{A}_2 + A_3)}{2 A z}$$

$$\phi_{12}(t) = \frac{\mu_0 A_1 m_1 A_2}{2 A z}$$

$$\phi_{13}(t) = \frac{\mu_0 A_1 m_1 A_3}{2 A z}$$

$$\phi_{14}(t) = \frac{\mu_0 A_1 m_1 A_4}{2 A z}$$



ponents only, namely, along gravity line and force component in the third direction is

dally between a minimum of zero when its maximum when its sub-pole is fully coupled

to phase-locked to rail.

is ignored.

### PERFORMANCE

ection indicated in Fig. 2b, flux linkages of be approximated to sinusoidal variation as case with each another and that  $\lambda_2$  &  $\lambda_1$  also (ature lag with  $\lambda_1$  &  $\lambda_2$  variations. The period

(1)

(2)

kage per phase, the ac coils are connected as y a quarter of a cycle, and that the dc coils components.

### M

idered excited with two components d.d.c.

( $\omega t + \theta$ )

(3)

( $\omega t + \theta$ )

(4)

Using Fig. 5a and denoting  $m_1, m_2, m_3$  and  $m_4$  to be the resultant mmf excitations around sub-poles 1, 2, 3 and 4 respectively, with positive sense when forcing flux to leave the sub-pole, then:

$$m_1(t) = -M_D - m_A(t) \quad (5)$$

$$m_2(t) = -M_D + m_A(t) \quad (6)$$

$$m_3(t) = M_D + m_B(t) \quad (7)$$

$$m_4(t) = M_D - m_B(t) \quad (8)$$

### Energized Sub-polar Areas for TRHSM

With  $A_1, A_2, A_3$  and  $A_4$  defined as above, then these areas vary trapezoidally as shown in Fig. 4a during the rail motion indicated in Fig. 2b. Note that the sum of any two adjacent areas is constant and equals  $A$ .

For simplicity, these trapezoidal variations are assumed sinusoids between a maximum of  $A$  and a minimum of zero as shown by the dotted lines in Fig. 2b. The equations describing these approximations are:

$$A_1(t) = (A/2)[1 + \cos(\omega t + \pi/4)] \quad (9)$$

$$A_2(t) = (A/2)[1 - \cos(\omega t + \pi/4)] \quad (10)$$

$$A_3(t) = (A/2)[1 + \cos(\omega t - \pi/4)] \quad (11)$$

$$A_4(t) = (A/2)[1 - \cos(\omega t - \pi/4)] \quad (12)$$

This approximation will give a maximum deviation error at trapezoidal corners of about 18%. However, the sum of areas constituting portions of adjacent sub-poles is still constant.

### Magnetic Sub-polar Fluxes for TRHSM

Let  $\phi_{11}, \phi_{12}, \phi_{13}, \phi_{14}, \phi_{21}, \phi_{22}, \phi_{23}, \phi_{24}, \phi_{31}, \phi_{32}, \phi_{33}, \phi_{34}, \phi_{41}, \phi_{42}, \phi_{43}, \phi_{44}, \phi_1, \phi_2, \phi_3$  &  $\phi_4$  be as defined above. Hence, each of  $m_1, m_2, m_3$  and  $m_4$  mmfs is driving an associated magnetic circuit similar to that shown in Fig. 6. Hence:

$$\phi_{11}(t) = \frac{\mu_0 A_1 m_1 (A_2 + A_3 + A_4)}{2 A z}$$

$$\phi_{12}(t) = \frac{\mu_0 A_1 m_1 A_2}{2 A z}$$

$$\phi_{13}(t) = \frac{\mu_0 A_1 m_1 A_3}{2 A z}$$

$$\phi_{14}(t) = \frac{\mu_0 A_1 m_1 A_4}{2 A z}$$

Similarly:

$$\begin{aligned}\phi_{22}(t) &= \frac{\mu_0 A_2 m_2 (A_1 + A_3 + A_4)}{2 A z} \\ \phi_{21}(t) &= \frac{\mu_0 A_2 m_2 A_1}{2 A z} \\ \phi_{23}(t) &= \frac{\mu_0 A_2 m_2 A_3}{2 A z} \\ \phi_{24}(t) &= \frac{\mu_0 A_2 m_2 A_4}{2 A z}\end{aligned}$$

Likewise:

$$\begin{aligned}\phi_{33}(t) &= \frac{\mu_0 A_3 m_3 (A_1 + A_2 + A_4)}{2 A z} \\ \phi_{31}(t) &= \frac{\mu_0 A_3 m_3 A_1}{2 A z} \\ \phi_{32}(t) &= \frac{\mu_0 A_3 m_3 A_2}{2 A z} \\ \phi_{34}(t) &= \frac{\mu_0 A_3 m_3 A_4}{2 A z}\end{aligned}$$

Finally:

$$\begin{aligned}\phi_{44}(t) &= \frac{\mu_0 A_4 m_4 (A_1 + A_2 + A_3)}{2 A z} \\ \phi_{41}(t) &= \frac{\mu_0 A_4 m_4 A_1}{2 A z} \\ \phi_{42}(t) &= \frac{\mu_0 A_4 m_4 A_2}{2 A z} \\ \phi_{43}(t) &= \frac{\mu_0 A_4 m_4 A_3}{2 A z}\end{aligned}$$

Hence, applying superposition theorem to find the fluxes  $\phi_1(t), \phi_2(t), \phi_3(t)$  &  $\phi_4(t)$  leaving sub-poles 1, 2, 3 and 4 respectively due to all mmfs of  $m_1, m_2, m_3$  and  $m_4$ ; then:

$$\phi_1(t) = \phi_{11} - \phi_{21} - \phi_{31} - \phi_{41}$$

Using the above equations for  $\phi_{11}, \phi_{21}, \phi_{31}$  &  $\phi_{41}$  respectively and rearranging, then:

$$\phi_1(t) = \frac{\mu_0 A_1 [A_2 (m_1 - m_2) + A_3 (m_1 - m_3) + A_4 (m_1 - m_4)]}{2 A z}$$

Using eqs. 5, 6, 7 & 8 for  $m_1, m_2, m_3$  &  $m_4$  and rearranging them:

$$\phi_1(t) = \frac{-\mu_0 A_1 [2 M_D (A_3 + A_4) + m_A (2 A_2 + A_3 + A_4) + m_B (A_3 - A_4)]}{2 A z}$$

Using eqs. 10, 11 & 12 for  $A_2, A_3$  &  $A_4$  and simplifying, then:

$$\phi_1(t) = \frac{-\mu_0 A_1 [2 M_D + m_A [2 - \cos(\omega t + \pi/4)] + m_B \cos(\omega t - \pi/4)]}{2 z}$$

Using eqs. 3 & 4 for  $m_A(t)$  and  $m_B(t)$  respective

$$\phi_1(t) = \frac{-\mu_0 A_1 [2 M_D + 2 m_A + m_B]}{2 z}$$

Similarly:  $\phi_2, \phi_3$  &  $\phi_4$  can be found to be:

$$\phi_2(t) = \frac{-\mu_0 A_2 [2 M_D - 2 m_A + m_B]}{2 z}$$

$$\phi_3(t) = \frac{\mu_0 A_3 [2 M_D + 2 m_B - m_A]}{2 z}$$

$$\phi_4(t) = \frac{\mu_0 A_4 [2 M_D - 2 m_B - m_A]}{2 z}$$

### Magnetic Sub-polar Flux Densities for TRLL

From the above equations, the sub-polar flux d

$$B_1(t) = \frac{\phi_1(t)}{A_1(t)} = \frac{-\mu_0 [2 M_D + 2 m_A]}{A_1(t)}$$

$$B_2(t) = \frac{\phi_2(t)}{A_2(t)} = \frac{-\mu_0 [2 M_D - 2 m_A]}{A_2(t)}$$

$$B_3(t) = \frac{\phi_3(t)}{A_3(t)} = \frac{\mu_0 [2 M_D + 2 m_B]}{A_3(t)}$$

$$B_4(t) = \frac{\phi_4(t)}{A_4(t)} = \frac{\mu_0 [2 M_D - 2 m_B]}{A_4(t)}$$

### Magnetic Lift Force for TRLLHSM

The TRLLHSM will exert a lift force,  $F_r$ , in order to energized air-gap,  $z$ . This lift force is composed of the magnetic flux densities  $B_i$  above which air is energized, and the sub-polar areas  $A_i$  above which air is energized, and the sub-polar flux densities  $B_i$ . Hence,  $F_r$  is given by:

$$F_r(t) = \sum_{i=1}^4 \frac{A_i B_i^2}{2 \mu_0}$$

Using eqs. 9, 10, 11 & 12 for  $A_1, A_2, A_3$  &  $A_4$ ; eqs. 17 & 18 with the aid of eqs. 3 & 4 for  $m_A$  &  $m_B$ ; then  $F_r$  is

$$F_r(t) = \frac{\mu_0 A [8 M_D^2 + 3 m^2 + 8 M_D m \cos(\omega t - \pi/4)]}{8 z}$$

Using eqs. 3&4 for  $m_A(t)$  and  $m_B(t)$  respectively, and simplifying; then:

$$\phi_1(t) = \frac{-\mu_0 A_1 [2 M_D + 2 m_A + m \sin(2\omega t + \theta - \pi/4)]}{2z} \quad (13)$$

Similarly,  $\phi_2, \phi_3$  &  $\phi_4$  can be found to be:

$$\phi_2(t) = \frac{-\mu_0 A_2 [2 M_D - 2 m_A + m \sin(2\omega t + \theta - \pi/4)]}{2z} \quad (14)$$

$$\phi_3(t) = \frac{\mu_0 A_3 [2 M_D + 2 m_B - m \sin(2\omega t + \theta - \pi/4)]}{2z} \quad (15)$$

$$\phi_4(t) = \frac{\mu_0 A_4 [2 M_D - 2 m_B - m \sin(2\omega t + \theta - \pi/4)]}{2z} \quad (16)$$

### Magnetic Sub-polar Flux Densities for TRLHSM

From the above equations, the sub-polar flux densities are found as:

$$B_1(t) = \frac{\phi_1(t)}{A_1(t)} = \frac{-\mu_0 [2 M_D + 2 m_A + m \sin(2\omega t + \theta - \pi/4)]}{2z} \quad (17)$$

$$B_2(t) = \frac{\phi_2(t)}{A_2(t)} = \frac{-\mu_0 [2 M_D - 2 m_A + m \sin(2\omega t + \theta - \pi/4)]}{2z} \quad (18)$$

$$B_3(t) = \frac{\phi_3(t)}{A_3(t)} = \frac{\mu_0 [2 M_D + 2 m_B - m \sin(2\omega t + \theta - \pi/4)]}{2z} \quad (19)$$

$$B_4(t) = \frac{\phi_4(t)}{A_4(t)} = \frac{\mu_0 [2 M_D - 2 m_B - m \sin(2\omega t + \theta - \pi/4)]}{2z} \quad (20)$$

### Magnetic Lift Force for TRLHSM

The TRLHSM will exert a lift force,  $F_r$ , in order to minimize its reluctance by minimizing the energized air-gap,  $z$ . This lift force is composed of several parts, according to the sub-polar areas,  $A_i$  above which air is energized, and according to the energizing magnetic flux densities,  $B_i$ . Hence,  $F_r$  is given by:

$$F_r(t) = \sum_{i=1}^4 \frac{A_i B_i^2}{2\mu_0}$$

Using eqs. 9, 10, 11 & 12 for  $A_1, A_2, A_3$  &  $A_4$ ; eqs. 17, 18, 19 & 20 for  $B_1, B_2, B_3$  &  $B_4$ ; and simplifying with the aid of eqs. 3 & 4 for  $m_A$  &  $m_B$ ; then  $F_r$  may be found as:

$$F_r(t) = \frac{\mu_0 A [8 M_D^2 + 3 m^2 + 8 M_D m \cos(\theta - \pi/4) + m^2 \sin(4\omega t + 2\theta)]}{8z^2}$$

Hence, the lift force,  $F_v$ , of TRLHSM is composed of two components: one steady which is supposed to support the boggie weight,  $W$ , via field control; and the other pulsating at four times the synchronous frequency.

Writing the mechanical equation of motion for the TRLHSM suspension boggie shown in Fig. 1b, then:

$$F_v - W = W \alpha_{vp}$$

Hence, the above two equations give:

1. the condition for stable field excitation,  $M_D(\theta, m)$ , at any ac excitation parameters of  $\theta$  &  $m$  as:

$$\frac{\mu_0 A [8 M_D^2 + 3 m^2 + 8 M_D m \cos(\theta - \pi/4)]}{8 z^2} = W \quad (21)$$

2. the resulting lift acceleration pulsation,  $\alpha_{vp}$ , at any ac excitation parameters of  $\theta$  &  $m$  as:

$$\alpha_{vp}(\theta, m, t) = \frac{\mu_0 A m^2 \sin(4\omega t + 2\theta)}{8 z^2 W} \quad (22)$$

### Open Circuit Voltages for TRLHSM

The open circuit induced voltage,  $E_A$ , at phase A coil terminals can be seen from Fig. 5a to be:

$$E_A(t) = N \frac{d}{dt} [\phi_2 - \phi_1]_{m=0}$$

Using eqs. 9, 10, 13 & 14 for  $A_1, A_2, \phi_1$  &  $\phi_2$  and simplifying, then:

$$E_A(t) = \frac{-\mu_0 \omega A M_D N \sin(\omega t + \pi/4)}{z} \quad (23)$$

Similarly, the open circuit induced voltage,  $E_B$ , at phase B coil terminals can be found to be:

$$E_B(t) = \frac{-\mu_0 \omega A M_D N \sin(\omega t - \pi/4)}{z} \quad (24)$$

### Magnetic Thrust Force for TRLHSM

The TRLHSM thrust force,  $F_h$ , can be obtained using the energy principle. Assuming ideal conversion, then:

$$F_h u = E_A i_A + E_B i_B$$

Using eqs. 2, 3, 4, 23 & 24 for  $\omega, i_A, i_B, E_A$  &  $E_B$ ; this simplifies to:

$$F_h(t) = \frac{\mu_0 \pi A M_D m \sin(\theta - \pi/4)}{2 p z} \quad (25)$$

Hence; the thrust force,  $F_h$ , is composed of the ZLHSM developed by West[3]. In his one steady and the other pulsating at twice

Eq. 25 shows that the TRLHSM will propel and brake within  $(-\frac{3\pi}{4}, \frac{\pi}{4})$ . This is due to the TRLHSM can be used either for motor or for braking with kinetic power converted to TRLHSM is virtually exerting zero force.

### Maximum Steady Thrusting Acceleration

The steady thrusting acceleration,  $\alpha_{hs}$ , related to the steady thrusting force,  $F_{hs}$ , by dividing

$$\alpha_{hs}(\theta, m) = \frac{\mu_0 \pi A M_D(\theta, m)}{2 p W}$$

where  $M_D(\theta, m)$  is an implicit function of  $\theta$  &  $m$

The maximum of  $\alpha_{hs}(\theta, m)$  for a given  $\theta$  occurs at  $m = \bar{m}(\theta)$  to give:

$$\bar{M}_D(\theta) = M_D(\theta, \bar{m}(\theta))$$

$$\bar{m}(\theta) = 2 z \sqrt{\frac{W}{\mu_0 A [3 + \sqrt{1 + 8 W z^2}]}}$$

$$\alpha_{hs}(\theta) = \alpha_{hs}(\theta, \bar{m}(\theta)) = \frac{\mu_0 \pi A \bar{M}_D(\theta)}{2 p W}$$

On the other hand, the maximum of  $\alpha_{hs}(\theta)$  occurs at  $\theta = \bar{\theta}$  to be:

$$\bar{\theta} = \frac{\pi}{4} \pm (\pi - \cos^{-1} \frac{1}{3})$$

This would split into two values:

$$\bar{\theta}_+ = \frac{5\pi}{4} - \cos^{-1} \frac{1}{3} = 3.3$$

where  $\bar{\theta}_+ \in (\frac{\pi}{4}, \frac{5\pi}{4})$ , the motoring range discussed for thrusting acceleration:

$$\alpha_{hs}(\bar{\theta}_+) = \frac{\pi z}{\sqrt{2} p}$$

and:

$$\bar{\theta}_- = \frac{5\pi}{4} + \cos^{-1} \frac{1}{3} = 4.542 \text{ rad}$$

used of two components: one steady which is field control; and the other pulsating at four

for the TRLHSM suspension boggie shown in

up

$M_D(\theta, m)$ , at any ac excitation parameters of

$$\frac{m \cos(\theta - \pi/4)}{3z^2} = W \quad (21)$$

$\gamma_{np}$ , at any ac excitation parameters of  $\theta$  &  $m$

$$\frac{\sin(\omega t + 2\theta)}{3z^2 W} \quad (22)$$

A coil terminals can be seen from Fig. 5a to

$$\phi_1, m=0$$

simplifying, then:

$$\sin(\omega t + \pi/4) \quad (23)$$

at phase B coil terminals can be found to be:

$$\sin(\omega t - \pi/4) \quad (24)$$

ed using the energy principle. Assuming ideal

$$E_B i_B$$

is simplifies to:

$$\frac{1}{z} \dots \quad (25)$$

0

Hence; the thrust force,  $F_h$ , is composed only of one steady component; an advantage over the ZLHSM developed by West[3]. In his machine, West has had two force components one steady and the other pulsating at twice the synchronous frequency.

Eq. 25 shows that the TRLHSM will propel when the current phase angle is within  $(\frac{\pi}{4}, \frac{5\pi}{4})$  and brake within  $(\frac{-2\pi}{4}, \frac{\pi}{4})$ . This is due to the mechanical and electrical system lags. The TRLHSM can be used either for motoring with electric power converted to kinetic or for braking with kinetic power converted to electric. At two  $\theta$  values, namely:  $\frac{\pi}{4}$  &  $\frac{5\pi}{4}$ , the TRLHSM is virtually exerting zero force.

### Maximum Steady Thrusting Acceleration for TRLHSM

The steady thrusting acceleration,  $\alpha_{hs}$ , relative to gravity could be obtained from eq. 25 for the steady thrusting force,  $F_{hs}$ , by dividing by the supported weight,  $W$ . Hence :

$$\alpha_{hs}(\theta, m) = \frac{\mu_0 \pi A M_D(\theta, m) m \sin(\theta - \pi/4)}{2pWz} \quad (26)$$

where  $M_D(\theta, m)$  is an implicit function of  $\theta$  &  $m$ .

The maximum of  $\alpha_{hs}(\theta, m)$  for a given  $\theta$  occurs at  $\bar{m}(\theta)$ . This could be found using eqs. 21 & 26 to give:

$$\bar{M}_D(\theta) = M_D(\theta, \bar{m}(\theta)) = \sqrt{\frac{3}{8}} \bar{m}(\theta) \quad (27)$$

$$\bar{m}(\theta) = 2z \sqrt{\frac{W}{\mu_0 A [3 + \sqrt{6} \cos(\theta - \pi/4)]}} \quad (28)$$

$$\alpha_{hs}(\theta) = \alpha_{hs}(\theta, \bar{m}(\theta)) = \frac{\pi z \sin(\theta - \pi/4)}{p[\sqrt{6} + 2 \cos(\theta - \pi/4)]} \quad (29)$$

On the other hand, the maximum of  $\alpha_{hs}(\theta)$  occurs at  $\bar{\theta}$ . This could be found using eq. 29 to be:

$$\bar{\theta} = \frac{\pi}{4} \pm (\pi - \cos^{-1} \sqrt{\frac{2}{3}}) \quad (30)$$

This would split into two values:

$$\bar{\theta}_+ = \frac{5\pi}{4} - \cos^{-1} \sqrt{\frac{2}{3}} = 3.312 \text{ rad} = 190^\circ$$

where  $\bar{\theta}_+ \in (\frac{\pi}{4}, \frac{5\pi}{4})$ , the motoring range discussed earlier giving the following maximum thrusting acceleration:

$$\alpha_{hs}(\bar{\theta}_+) = \frac{\pi z}{\sqrt{2} p}$$

and:

$$\bar{\theta}_- = \frac{5\pi}{4} + \cos^{-1} \sqrt{\frac{2}{3}} = 4.542 \text{ rad} = 260^\circ$$

with  $\bar{\theta}_- \in (-\frac{3\pi}{4}, \frac{\pi}{4})$ , the generation range discussed earlier, giving the following maximum braking deceleration:

$$\alpha_{hs}(\bar{\theta}_-) = \frac{-\pi z}{\sqrt{2} p}$$

Hence, the maximum value of  $\alpha_{hs}$  is given by:

$$\alpha_{hsr} = |\alpha_{hs}(\bar{\theta})| = \frac{\pi z}{\sqrt{2} p} \quad (31)$$

Substituting either  $\bar{\theta}$  values in eqs. 28 & 27 for  $\bar{m}$  &  $\bar{M}_D$  gives:

$$\bar{m} = 2z \sqrt{\frac{W}{\mu_0 A}} \quad (32)$$

and:

$$\bar{M}_D = z \sqrt{\frac{3W}{2\mu_0 A}} \quad (33)$$

#### Lift Pulsating Acceleration for TRLHSM

Eq. 22 can provide a scale for the magnitude of lift acceleration pulsation,  $\alpha_{vz}$ , the worst of which is  $\alpha_{vz}$  occurring at  $\bar{\theta}$  &  $\bar{m}$ . Hence, using eqs. 30 & 32 for  $\bar{\theta}$  &  $\bar{m}$ , this gives:

$$\alpha_{vz}(t) = \alpha_{vz}(\bar{\theta}, \bar{m}) = \frac{1}{2} \sin(4\omega t + 2\bar{\theta}) \quad (34)$$

This means that the worst pulsation in lift acceleration is half that of gravity in magnitude and running at four times the synchronous frequency.

#### Thrust Pulsating Acceleration for TRLHSM

It was mentioned earlier that the thrust pulsating acceleration,  $\alpha_{hr}$ , is zero. Hence:

$$\alpha_{hr}(t) = 0 \quad (35)$$

### REVIEW ANALYSIS OF ZZLHSM PERFORMANCE

#### Coil Connections for ZZLHSM

When the rail of ZZLHSM moves in the direction indicated in Fig. 2a, flux linkages of ac coils will assume linear segments and can be approximated to sinusoidal variation as shown in Fig. 4b. The period of these variations is given by:

$$T' = \frac{2}{\omega'}$$

with angular frequency,  $\omega'$ , given by:

$$\omega' = \frac{\pi}{I}$$

Hence, to obtain maximum variation in flux as shown in Fig. 5b.

#### Magnetic Sub - polar Excitations for ZZLHSM

With treatment similar to that of TRLHSM be given as:

$$m'_1(t) = -m'_2(t) = -$$

$$m'_2(t) = -m'_1(t) = -$$

where  $m'_A(t)$  is given by:

$$m'_A(t) = N i'_A(t) = m$$

#### Energized Sub - polar Areas for ZZLHSM

The ZZLHSM sub-polar areas vary triangularly indicated in Fig. 2a. These variations are as

$$A'_1(t) = A'_3(t) = (A/2)$$

$$A'_2(t) = A'_4(t) = (A/2)$$

This approximation will give a maximum d

#### Magnetic Sub - polar Fluxes for ZZLHSM

With similar treatment to that of TRLHSM

$$\phi'_1(t) = -\phi'_3(t) = \frac{-\mu_0 \cdot}{2}$$

$$\phi'_2(t) = -\phi'_4(t) = \frac{-\mu_0 \cdot}{2}$$

#### Magnetic Sub - polar Flux Densities for ZZLHSM

These are given by:

$$B'_1(t) = -B'_3(t) = \frac{-\mu_0 \cdot}{2}$$

earlier, giving the following maximum

(31)

$r_D$  gives:

(32)

acceleration pulsation,  $\alpha_{vp}$ , the worst of

(34)

tion is half that of gravity in magnitude

acceleration,  $\alpha_{hf}$ , is zero. Hence:

(35)

NCE

n indicated in Fig. 2a, flux linkages of approximated to sinusoidal variation as given by:

$$T' = \frac{2p}{u} \tag{36}$$

with angular frequency,  $\omega'$ , given by:

$$\omega' = \frac{\pi u}{P} \tag{37}$$

Hence, to obtain maximum variation in flux linkage per phase, the ac coils are connected as shown in Fig. 5b.

Magnetic Sub - polar Excitations for ZZLHSM

With treatment similar to that of **TRLHSM**, then the sub-poles excitations in Fig. 5b could be given as:

$$m'_1(t) = -m'_3(t) = -M'_D - m'_A(t) \tag{38}$$

(33)

$$m'_2(t) = -m'_4(t) = -M'_D + m'_A(t) \tag{39}$$

where  $m'_A(t)$  is given by:

$$m'_A(t) = N i'_A(t) = m' \cos(\omega' t + \theta') \tag{40}$$

Energized Sub - polar Areas for ZZLHSM

The ZZLHSM sub-polar areas vary triangularly as shown in Fig. 4b during the rail motion indicated in Fig. 2a. These variations are assumed sinusoids with equations given by:

$$A'_1(t) = A'_3(t) = (A/2)[1 + \cos(\omega' t)] \tag{41}$$

$$A'_2(t) = A'_4(t) = (A/2)[1 - \cos(\omega' t)] \tag{42}$$

This approximation will give a maximum deviation error near corners of about 21%.

Magnetic Sub - polar Fluxes for ZZLHSM

With similar treatment to that of **TRLHSM**, then these fluxes are given by:

$$\phi'_1(t) = -\phi'_3(t) = \frac{-\mu_0 A'_1 (M'_D + m'_A)}{z} \tag{43}$$

$$\phi'_2(t) = -\phi'_4(t) = \frac{-\mu_0 A'_2 (M'_D - m'_A)}{z} \tag{44}$$

Magnetic Sub - polar Flux Densities for ZZLHSM

These are given by:

$$B'_1(t) = -B'_3(t) = \frac{-\mu_0 (M'_D + m'_A)}{z} \tag{45}$$

$$B_2'(t) = -B_4'(t) = \frac{-\mu_0 (M_D' - m_A')}{z} \quad (46)$$

### Magnetic Lift Force for ZZLHSM

This is found, in a similar way to that of TRLHSM, as:

$$F_v'(t) = \frac{\mu_0 A [2 M_D'^2 + m'^2 + 2 M_D' m' \cos(\theta') + m'^2 \cos(2\omega' t + 2\theta') + 2 M_D' m' \cos(2\omega' t + \theta')]}{2 z^2}$$

Hence, the lift force,  $F_v'$ , of ZZLHSM is composed of a steady component restricting  $M_D'(\theta', m')$ , at any ac excitation parameters of  $\theta'$  &  $m'$  to satisfy:

$$\frac{\mu_0 A [2 M_D'^2 + m'^2 + 2 M_D' m' \cos(\theta')]}{2 z^2} = W \quad (47)$$

and a pulsation one given by:

$$\alpha_{v,p}'(\theta', m', t) = \frac{\mu_0 A m' [2 M_D' \cos(2\omega' t + \theta') + m' \cos(2\omega' t + 2\theta')]}{2 z^2 W} \quad (48)$$

### Open Circuit Voltage for ZZLHSM

This is found to be:

$$E_A'(t) = \frac{-2\mu_0 \omega' A M_D' N \sin(\omega' t)}{z} \quad (49)$$

### Magnetic Thrust Force for ZZLHSM

This is given as:

$$F_h'(t) = \frac{\mu_0 \pi A M_D' m' [\sin(\theta') - \sin(2\omega' t + \theta')]}{p z} \quad (50)$$

and is composed of two components: one steady and the other pulsating at twice the synchronous frequency. Note that when the rail completely links sub-poles 1&3 or 2&4, then  $\omega' t = \text{integral multiple of } \pi$  giving  $F_h'$  zero. This is why ZZLHSM needs a starter.

### Maximum Steady Thrusting Acceleration for ZZLHSM

This is given as:

$$\alpha_{h,s}'(\theta', m') = \frac{\mu_0 \pi A M_D'(\theta', m') m' \sin(\theta')}{p W z} \quad (51)$$

Hence, the ZZLHSM will propel when the current phase angle is within  $(0, \pi)$  and will brake within  $(-\pi, 0)$ .

The maximum of  $\alpha_{h,s}'(\theta', m')$  for a given  $\theta'$  occurs at:

$$\overline{M}_D'(\theta') = M_D'(\theta', \overline{m}')$$

$$\overline{m}'(\theta') = \sqrt{\frac{\sqrt{z}}{\mu_0 A [\sqrt{z}]}}$$

$$\alpha_{h,s}'(\theta') = \alpha_{h,s}'(\theta', \overline{m}'(\theta')) :$$

On the other hand, the maximum of  $\alpha_{h,s}'(\theta')$

$$\overline{\theta}' = \pm \frac{3\pi}{4}$$

This would split into two values:

$$\overline{\theta}'_+ = \frac{3\pi}{4} \in (($$

in the motoring range discussed above, given:

$$\alpha_{h,s}'(\overline{\theta}'_+) =$$

and:

$$\overline{\theta}'_- = \frac{-3\pi}{4} \in ($$

in the generating range discussed above, given:

$$\alpha_{h,s}'(\overline{\theta}'_-) =$$

Hence, the maximum value of  $\alpha_{h,s}'$  is given by:

$$\alpha_{h,s,z}' = |\alpha_{h,s}'(\overline{\theta}'_+)|$$

with:

$$\overline{m}' = z \sqrt{\frac{z}{\mu_0}}$$

and:

$$\overline{M}_D' = z \sqrt{\frac{z}{\mu_0}}$$

### Lift Pulsating Acceleration for ZZLHSM

Eq. 48 can provide a scale for the magnitude which is  $\alpha_{v,p}'$  occurring at  $\overline{\theta}'$  &  $\overline{m}'$ . Hence, use:

$$\alpha_{v,p,z}'(t) = \alpha_{v,p}'(\overline{\theta}', \overline{m}')$$



$$\frac{b - m'_A}{z} \quad (46)$$

ISM, as:

$$\frac{I^2 \cos(2\omega' t + 2\theta') + 2M'_D m' \cos(2\omega' t + \theta')}{2z^2}$$

posed of a steady component restricting  $I$  &  $m'$  to satisfy:

$$\frac{m' \cos(\theta')}{z} = W \quad (47)$$

$$\frac{I \cos(\theta') + m' \cos(2\omega' t + 2\theta')}{z^2 W} \quad (48)$$

$$I \sin(\omega' t) \quad (49)$$

$$- \sin(2\omega' t + \theta') \quad (50)$$

and the other pulsating at twice the syn- completely links sub-poles 1&3 or 2&4, then is why ZLHSM needs a starter.

### ZLHSM

$$\frac{m' \sin(\theta')}{z} \quad (51)$$

nt phase angle is within  $(0, \pi)$  and will brake

es at:

$$\overline{M}'_D(\theta') = M'_D(\theta', \overline{m}'(\theta')) = \frac{\overline{m}'(\theta')}{\sqrt{2}} \quad (52)$$

$$\overline{m}'(\theta') = \sqrt{\frac{\sqrt{2} W z^2}{\mu_0 A [\sqrt{2} + \cos(\theta')]}} \quad (53)$$

$$\alpha'_{hs}(\theta') = \alpha'_{hs}(\theta', \overline{m}'(\theta')) = \frac{\pi z \sin(\theta')}{p [\sqrt{2} + \cos(\theta')]} \quad (54)$$

On the other hand, the maximum of  $\alpha'_{hs}(\theta')$  occur at  $\overline{\theta}'$ . This is given as:

$$\overline{\theta}' = \pm \frac{3\pi}{4} \quad (55)$$

This would split into two values:

$$\overline{\theta}'_+ = \frac{3\pi}{4} \in (0, \pi)$$

in the motoring range discussed above, giving the following maximum thrusting acceleration:

$$\alpha'_{hs}(\overline{\theta}'_+) = \frac{\pi z}{p}$$

and:

$$\overline{\theta}'_- = \frac{-3\pi}{4} \in (-\pi, 0)$$

in the generating range discussed above, giving the following maximum braking deceleration:

$$\alpha'_{hs}(\overline{\theta}'_-) = \frac{-\pi z}{p}$$

Hence, the maximum value of  $\alpha'_{hs}$  is given by:

$$\alpha'_{hs\pi} = |\alpha'_{hs}(\overline{\theta}')| = \frac{\pi z}{p} \quad (56)$$

with:

$$\overline{m}' = z \sqrt{\frac{2W}{\mu_0 A}} \quad (57)$$

and :

$$\overline{M}'_D = z \sqrt{\frac{W}{\mu_0 A}} \quad (58)$$

### Lift Pulsating Acceleration for ZLHSM

Eq. 48 can provide a scale for the magnitude of lift acceleration pulsation,  $\alpha'_{vp}$ , the worst of which is  $\alpha'_{vp\pi}$  occurring at  $\overline{\theta}'$  &  $\overline{m}'$ . Hence, using Eqs. 55 & 57 for  $\overline{\theta}'$  &  $\overline{m}'$ , then:

$$\alpha'_{vp\pi}(t) = \alpha'_{vp}(\overline{\theta}', \overline{m}') = -\cos(2\omega' t) \quad (59)$$

This means that the worst pulsation in lift acceleration is equal to that of gravity in magnitude and running at twice the synchronous frequency.

#### Thrust Pulsating Acceleration for ZZLHSM

It could be seen from eqs. 50,55&56 that the worst magnitude of thrust acceleration pulsation,  $\alpha'_{hpz}$  is  $\alpha'_{hpz}$ , occurring at  $\bar{\theta}'$  &  $\bar{m}'$ , and is given by:

$$\alpha'_{hpz}(t) = -\sqrt{2} \sin(2\omega' t + \bar{\theta}') \quad (60)$$

This means that the worst pulsation in thrust acceleration is over 1.4 that of gravity in magnitude and running at twice the synchronous frequency.

#### CHARACTERISTICAL DIFFERENCES BETWEEN ZZLHSM AND TRLHSM

The ZZLHSM is a single phase linear machine that needs a starter. Its maximum thrusting acceleration is  $\pi z/p$  and this occurs at field excitation,  $M_D$ , of  $z \sqrt{W/(\mu_0 A)}$ ; armature excitation,  $m$ , of  $\sqrt{2} z \sqrt{W/(\mu_0 A)}$  with  $135^\circ$  phase. Pulsation in accelerations operates at twice the synchronous frequency with worst value relative to gravity of 1.0 in the lift direction and  $\sqrt{2}$  in the thrust direction.

On the other hand, The TRLHSM is a two-phase self-starting linear machine. Its maximum thrusting acceleration is  $\sqrt{0.5} \pi z/p$  and this occurs at field excitation,  $M_D$ , of  $\sqrt{1.5} z \sqrt{W/(\mu_0 A)}$ ; armature excitation,  $m$ , of  $2 z \sqrt{W/(\mu_0 A)}$  with  $190^\circ$  or  $260^\circ$  phase. Pulsation in accelerations operates at four times the synchronous frequency with worst value relative to gravity of 0.5 in the lift direction and 0.0 in the thrust direction.

#### CONCLUSION

For same speed, TRLHSM is advantageous over ZZLHSM in that it is self-starting, operating at half the switching frequency, having half the worst lift pulsation and no thrust pulsation at all.

On the other hand, ZZLHSM is advantageous over TRLHSM in that it is a single phase machine with  $\sqrt{2}$  gain in thrust acceleration involving  $\sqrt{0.5}$  less armature excitation and  $\sqrt{2/3}$  less field excitation.

Both machines pulsate at same frequency, but this is a second harmonic in ZZLHSM and a fourth in TRLHSM.

#### ACKNOWLEDGMENT

The author would like to express his thanks to Dr. S. Abu-Shadi at the electrical engineering department of King Abdul-Aziz University in Saudi Arabia for his valuable assistance and comments.

#### REFERENCES

- [1] McLean, G. W. & West, A. N. (1988) Using the Zig-Zag Synchronous Motor and for the Future, IMechE, pp.
- [2] McLean, G. W. (1988). Review Vol. 35, Part B, No. 6, pp. 380.
- [3] West, A. N. (1982). The Conductorless Linear Synchronous Motor. Ph.D Thesis, Elect. Engg. Dept.

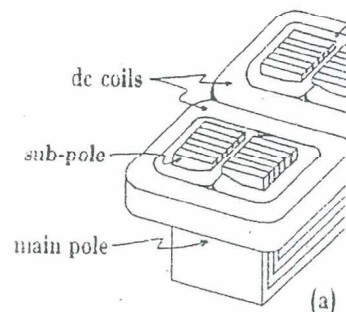


Fig. 1 (a) ZZLH

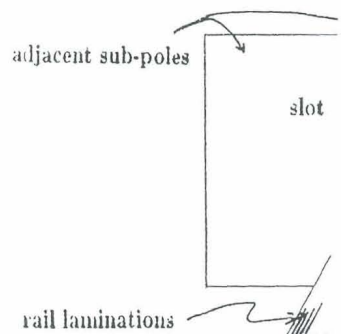


Fig. 3 Overlap

ion is equal to that of gravity in  
ency.

magnitude of thrust acceleration  
(60)

ation is over 1.4 that of gravity in  
ency.

ZZLHSM AND TRIHSM

is a starter. Its maximum thrusting  
n,  $M_D$ , of  $2\sqrt{W}/(\mu_0 A)$ ; armature  
ation in accelerations operates at  
relative to gravity of 1.0 in the lift

-starting linear machine. Its max-  
cures at field excitation,  $M_D$ , of  
with  $190^\circ$  or  $260^\circ$  phase. Pulsation  
quency with worst value relative  
st direction.

SM in that it is self-starting, oper-  
worst lift pulsation and no thrust

LHSM in that it is a single phase  
 $\sqrt{0.5}$  less armature excitation and

second harmonic in ZZLHSM and

u-Shadi at the electrical engineer-  
Arabia for his valuable assistance

REFERENCES

- [1] McLean, G. W. & West, A. N. (1984). Combined Lift and Thrust for Maglev Vehicles Using the Zig-Zag Synchronous Motor, Proc. Int. Conf. on Maglev Transport Now and for the Future, IMechE, pp. 87-97.
- [2] McLean, G. W. (1988). Review of Recent Progress in Linear Motors. IEE Proc., Vol. 35, Part B, No. 6, pp. 380-416.
- [3] West, A. N. (1982). The Control of a Linear Homopolar Synchronous Machine. PhD Thesis, Elect. Engg. Dept., Manchester University.

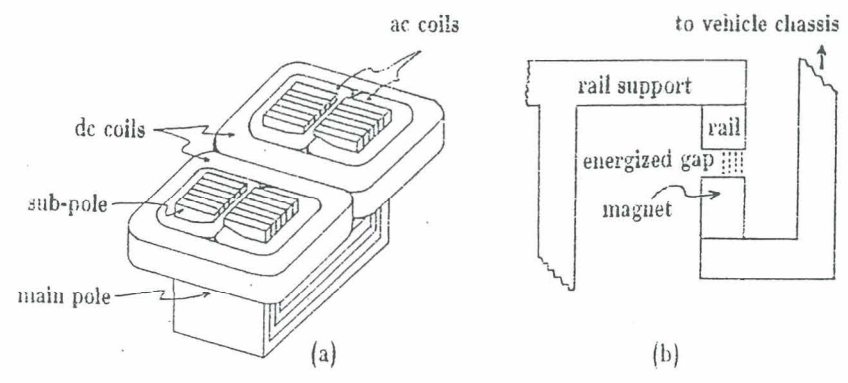


Fig. 1 (a) ZZLHSM magnet and (b) vehicle boggie

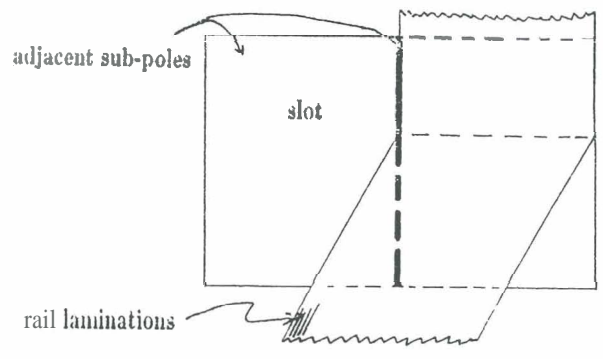


Fig. 3 Overlap area between rail and ZZLHSM sub-poles

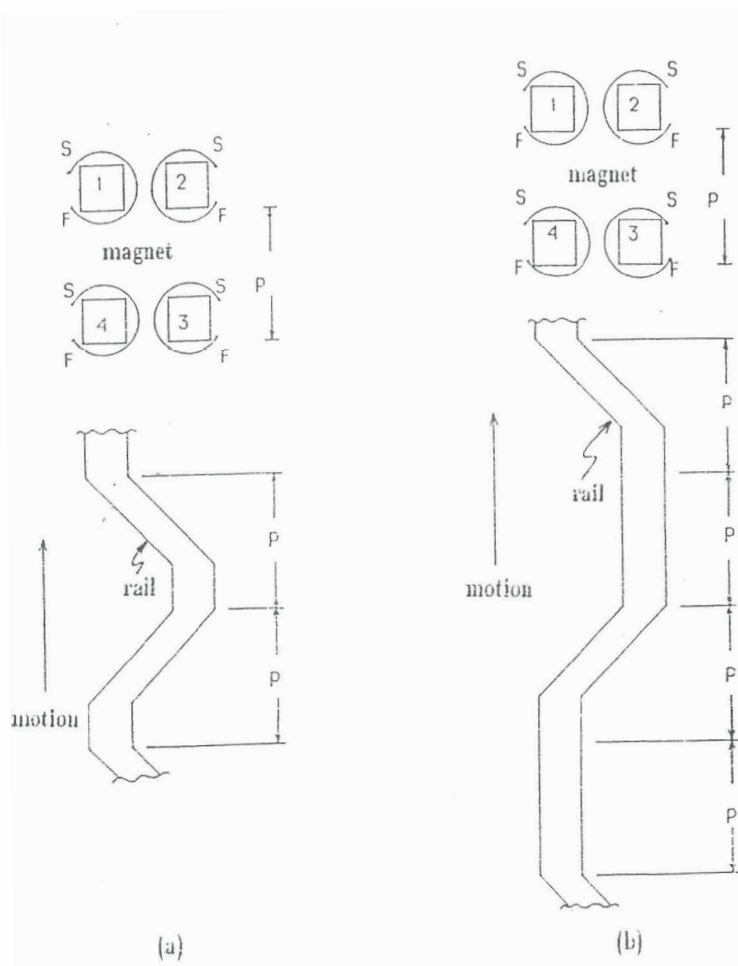


Fig. 2 Magnet and rail of (a) ZZLHSM and (b) TRLHSM

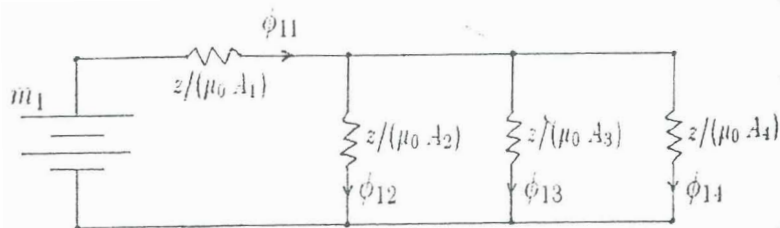


Fig. 6 The magnetic circuit driven by  $m_1$  around sub-pole 1

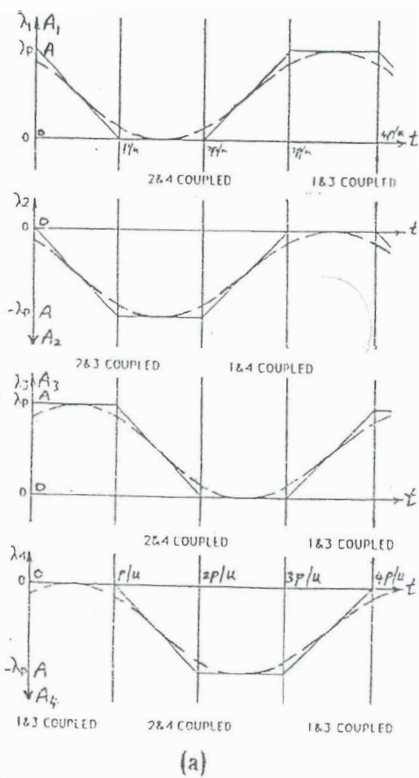


Fig. 4 Sub-polar flux-linkages and areas  $f$

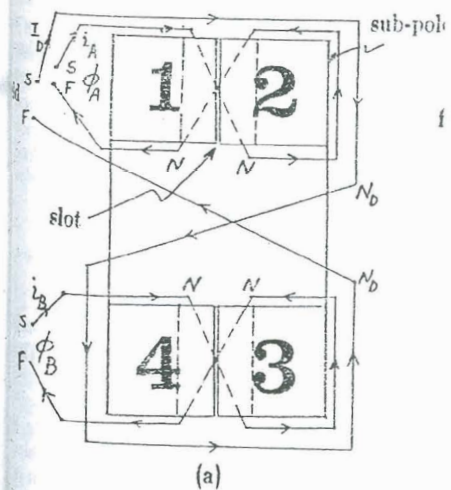


Fig. 5 Coil connections for (a)

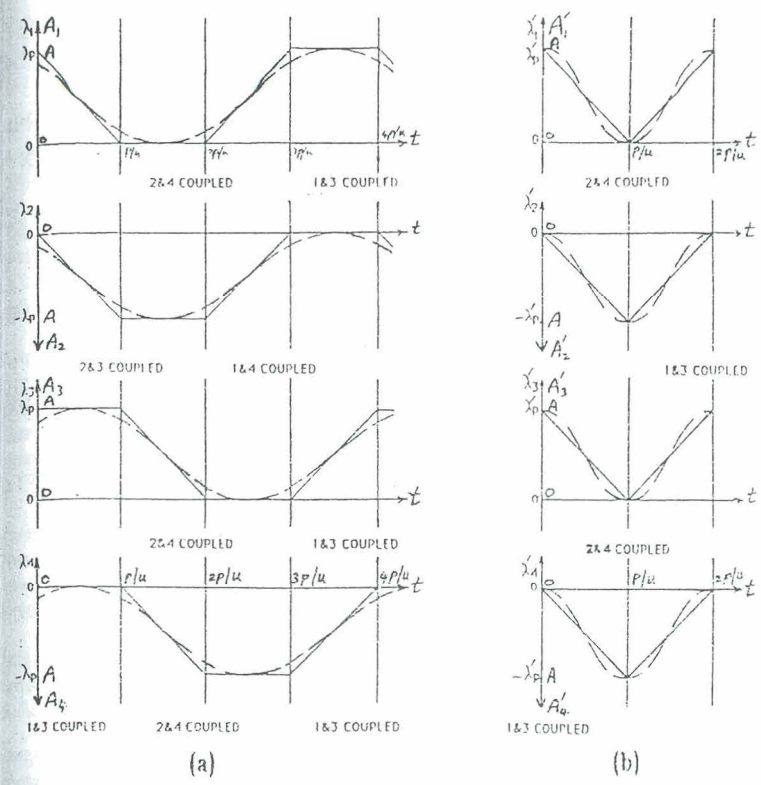
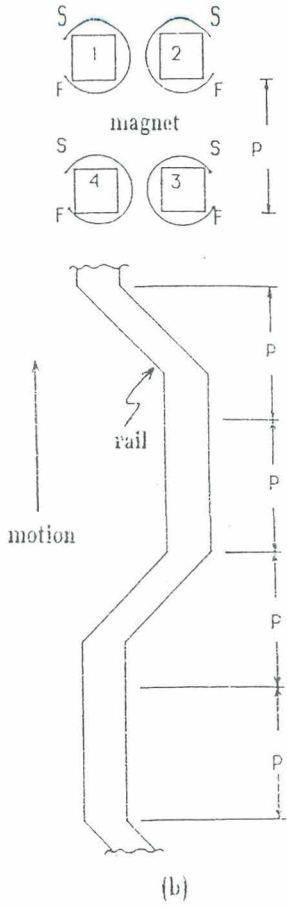


Fig. 4 Sub-polar flux-linkages and areas for (a) TRLHSM and (b) ZZLHSM

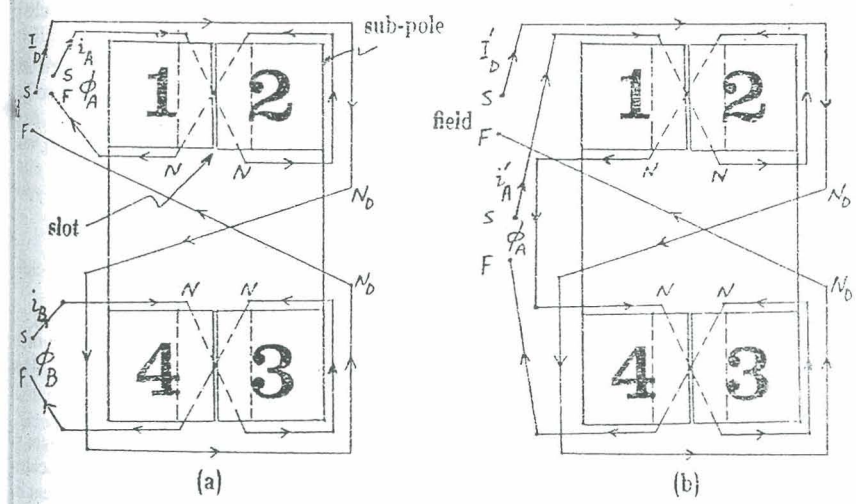
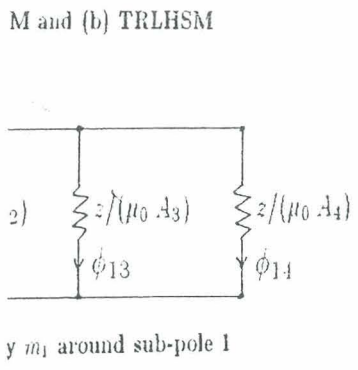


Fig. 5 Coil connections for (a) TRLHSM and (b) ZZLHSM